1

Stereotactic Body Radiotherapy for Pancreatic Adenocarcinoma: Set-Up Error Correction Using Internal Markers and Its Association with the Patient's Body Mass Index

Chi Lin, Shifeng Chen and Michael J. Baine
University of Nebraska Medical Center, USA

1. Introduction

Approximately 44,000 patients will develop new pancreatic cancers in the US in 2011 and 38,000 patients will die from the disease (ACS). Prognosis is directly related to the extent of tumor. The median survivals for these patients range from 11-18 months for those with localized disease, 10-12 months for those with locally advanced disease, and 5-7 months for those with metastatic disease, respectively (Evans DBAJ 2011). Although surgical resection is the only treatment associated with long-term survival, patients with resectable diseases usually account for only 20-25% of cases at diagnosis.

Despite resection, local regional recurrence and distant metastases occur in up to 50% of patients and two-year survival rates range from 20-40% with surgery alone. In 1974, the Gastrointestinal Tumor Study Group prospectively randomized patients after curative resection of pancreatic adenocarcinoma to adjuvant chemoradiation versus observation. The results of this study indicated a doubling of median and quadrupling of long-term survival with adjuvant chemoradiation (median, 20 vs. 11 months; 5-year survival, 19% vs. 5%). A US Intergroup study compared gemcitabine vs. infusional 5-FU chemotherapy for one month prior to and three months after chemoradiation, consisting of continuous infusional 5-FU, as adjuvant therapy after pancreatic cancer resection; outcome in those with tumor located in the pancreatic head was the primary study endpoint (Regine et al. 2008). The gemcitabine plus chemoradiation arm was superior to the 5-FU plus chemoradiation arm, with a median survival of 20.6 months vs. 16.9 months and survival at 3-years of 32% vs. 21%. This survival advantage came at a cost of appreciable toxicity, with grade 3-4 hematologic and non-hematologic toxicities occurring in 58% and 58% of subjects, respectively. Oettle et al compared gemcitabine given at 1000 mg/m² weekly for 3 of 4 weeks x 6 cycles to no additional therapy in 368 patients with resected pancreatic cancer (Oettle et al. 2007). Adjuvant gemcitabine was associated with a significant improvement in disease-free survival (13.4 vs 6.9 months), and a trend towards improvement in overall survival (median 22.1 vs 20.2 months); 34% of those receiving gemcitabine were alive at 3 yr vs. 20.5% with

surgery alone. Grade 3-4 hematologic and non-hematologic toxicities occurred in fewer than 5% of subjects receiving gemcitabine.

While these studies indicate improvement with adjuvant therapy, there is still need to improve upon these results. A disadvantage of adjuvant therapy is that as many as 25% of patients have their treatment either delayed or forgone due to post-operative complications (Yeo CJ 1997; Spitz et al. 1997; Klinkenbijl et al. 1999). In an effort to increase the number of patients receiving adjuvant therapy, chemotherapy and radiation therapy can be administered pre-operatively (neoadjuvantly) to potential surgical candidates. Additional potential benefits of pre-operative therapy include the delivery of therapy to well-oxygenated tissues, the potential to downstage tumors (particularly when the lesion is borderline resectable or unresectable because of regional factors such as tumor involvement of the superior mesenteric vein or portal vein, or tumor abutment/encasement of the superior mesenteric artery or celiac trunk or gastroduodenal artery up to hepatic artery), and the opportunity to observe patients for the development of metastatic disease during therapy. After maximal tumor shrinkage and no interval development of metastatic disease, surgery can be considered.

The current standard neoadjuvant regimen includes several months of chemotherapy followed by 5 – 6 weeks of radiation therapy concurrent with radiation sensitizing chemotherapy, followed by a 4 - 6 week therapy break prior to surgery. This chemoradiation regimen is fairly debilitating. ECOG (Pisters et al. 2000) conducted a phase II trial of preoperative conventional (50.4 Gy, 1.8 Gy/fraction) chemoradiation, showing that 51% of patients had toxicity-related hospital admissions. Treatment-related toxicities were found to be proportional to the irradiated volume and radiation dose. At M.D. Anderson, an accelerated radiotherapy schedule using 30 Gy in 10 fractions appeared to be more tolerable and equally effective (Breslin et al. 2001; Pisters et al. 1998). A recent randomized trial (Bujko et al. 2006) has compared preoperative short-course radiotherapy with preoperative conventionally fractionated chemoradiation for rectal cancer. The results showed no difference in actuarial 4-year overall survival (67.2% in the short-course group vs. 66.2% in the chemoradiation group, P = 0.960), disease-free survival (58.4% vs. 55.6%, P = 0.820), and crude incidence of local recurrence (9.0% vs. 14.2%, P = 0.170). The study also reported similar late toxicity (10.1% vs. 7.1%, P = 0.360) and higher early radiation toxicity in the chemoradiation group (18.2% vs. 3.2%, P < 0.001). These data suggest the equivalence in efficacy between short course and long course neoadjuvant therapy. Koong et al. (Koong et al. 2004) has conducted a phase I study of stereotactic radiosurgery in patients with unresectable pancreatic cancer. Fifteen patients were treated at 3 dose levels (3 patients received 15 Gy in 1 fraction, 5 patients received 20 Gy in 1 fraction, and 7 patients received 25 Gy in 1 fraction). No Grade 3 or higher acute GI toxicity was observed. In the 6 evaluable patients who received 25 Gy, the median survival was 8 months. All patients in the study had local control until death or progressed systemically as the site of first progression. This study suggests the feasibility of stereotactic radiosurgery in pancreatic cancer.

Following the methodology of Koong et al, one can apply the linear-quadratic formulism for radiation cell killing to "equate" schemes that vary the dose/fraction and number of fractions. This concept of biologically equivalent dose says that the total effect is given by:

$$(nd)\left\{1+d\Big/\frac{\alpha}{\beta}\right\}$$

Where n is the # of fractions and d is the dose/fraction. The "alpha-beta ratio" characterizes the radiation response of a particular tissue; a higher value is indicative of a tissue that responds acutely to the effects of radiation. Due to their highly proliferative nature, most tumors fall into this category. Because prolonging the treatment time introduces a sparing (repair) effect in acutely responding tissues, there is significant motivation to deliver radiation in larger fractions over a shorter time.

As the duodenum is in closest proximity to the majority of the pancreatic head tumors, it is impossible to avoid treating this structure to a relatively high radiation dose. Koong et al's data suggests that it is possible to irradiate a small volume of duodenum to a dose of 22.5 Gy in one fraction with acceptable toxicity. While the dose-fractionation scheme employed by Koong et al resulted in no significant morbidity, we proposed a phase I study of hypofractionated stereotactic body radiotherapy as part of a neoadjuvant regimen in patients with locally advanced pancreatic cancer using a more conservative starting dose of 5 Gy x 5.

The types of geometric uncertainties that should be considered in stereotactic body radiotherapy include tumor motion and patient position (setup error). Discrepancies between the actual and planned positions of targets and organs-at-risk during stereotactic body radiotherapy can lead to reduced doses to the tumor and/or increased doses to normal tissues than planned, potentially reducing the local control probability and/or increasing toxicity. Therefore, accurate and precise target localization is critical for hypofractionated stereotactic body radiotherapy. Studies found that the bony anatomy is a poor surrogate for intraabdominal (Herfarth et al. 2000) and intrathoracic (Guckenberger et al. 2006; Sonke, Lebesque, and van Herk 2008) targets. Therefore, direct tumor localization is important. Unfortunately, soft tissues are not seen on Exac-Trac (BrainLAB, Heimstetten, Germany) X-ray images. Thus, fiducial markers for the pancreatic cancer are required. The purpose of the current study is to assess daily set-up error using the Exac-Trac system and implanted pancreatic fiducial markers during stereotactic body radiotherapy for patients with locally advanced pancreatic adenocarcinoma in the current ongoing institutional phase I study and to evaluate the effect of body mass index (BMI) on set-up error correction.

2. Methods

2.1 Patients

Included in this study are adult patients (≥ 19 years old) who had a Karnofsky performance status of ≥ 60 and underwent stereotactic body radiotherapy planning and treatment between October 2008 and February 2011 as part of an institutional research ethics board-approved study of neoadjuvant hypofractionated stereotactic body radiotherapy following chemotherapy in patients with borderline resectable or unresectable pancreatic adenocarcinoma. Daily isocenter positioning correction was investigated in 26 patients treated with 5 fractions of SBRT for locally advanced pancreatic cancer. Two fiducial markers were implanted into the pancreatic head approximately two centimeters apart. With daily Exac-Trac images, 3 dimensional couch shifts were made by matching corresponding fiducial markers to the digitally reconstructed radiograph from a simulation CT scan. BMI was calculated by Weight (kg)/Height^2 (m^2) and categorized into normal weight 18.5 -25 (kg/m^2) and overweight/obese >25 (kg/m^2).

2.2 Stereotactic body radiotherapy planning and treatment

2.2.1 Patient's positioning

The treatment position of the patient was supine, with their arms above their head. The immobilization device (Medical Intelligence blue bag) was molded into an immobilizing bed for the intended patient's entire body to make sure that the patients' position was the same during planning, simulation and treatment.

2.2.2 Patient data acquisition

A treatment planning free breathing CT scan with IV contrast was required to define tumor, clinical, and planning target volumes. A respiratory sorted treatment planning 4D CT scan was then acquired with the patient in the same position and immobilized using the same device as used for treatment. All tissues to be irradiated were included in the CT scan, with a slice thickness of 3 mm. Conventional MRI scans (T1 and T2) were included to assist in definition of target volumes. FDG PET-CT, if available, was also included in the treatment planning. The Gross Tumor Volume (GTV), Clinical Target Volume (CTV), Planning Target Volume (PTV), and organs-at-risk were outlined on all CT slices in which the structures exist.

2.2.3 Volumes

The GTV was defined as all known gross disease determined from CT, clinical information, endoscopic findings, FDG PET-CT and/or conventional MRI. The Integrated Tumor Volume based on CT/MRI/PET (GTV_{fusion}) was defined as gross disease on the free breathing CT scan, MRI scan and FDG-PET scan. These scans were correlated via image fusion technique. The volume was delineated by the treating physician on the above scans separately. The GTV_{CT}, GTV_{MRI} and GTV_{PET} (if done) were eventually fused together to generate GTV_{fusion}. Patients who had the maximal dimension of the GTV_{fusion} > 8 cm were not eligible for the study. The CTV was defined as the GTVs plus areas considered containing potential microscopic disease. In this study, we had no intension to treat the potential microscopic disease with stereotactic body radiotherapy, therefore the CTV was defined as GTVs (i.e. both the primary tumor and the lymph nodes containing clinical or radiographic evidence of metastases) plus areas between $GTV_{primary}$ and $GTV_{lymph\ nodes}$. The integrated CTV was created with 4D CT information to compensate for internal organ motion. The PTV provided a margin around integrated CTV to compensate for the variability of treatment set-up. Organs-at-Risk were defined as follows: the skin surface, the unspecified tissue (the tissue within the skin surface and outside all other critical normal structures and PTVs was designated as unspecified tissue), spinal cord (spinal cord contours were defined at least 5 mm larger in the radial dimension than the spinal cord itself, i.e. the cord diameter on any given slice was 10 mm larger than the cord itself), duodenum, stomach, liver, right kidney, left kidney, small bowels excluding duodenum, and spleen.

2.2.4 The treatment technique

The Novalis accelerator (BrainLAB, Heimstetten, Germany) was used to deliver stereotactic body radiotherapy. It incorporates stereotactic x-ray capabilities for verifying target position. This consists of two floor mounted x-ray tubes and two opposing amorphous

silicon flat panel detectors mounted to the ceiling. Each x-ray tube/detector pair is configured to image through the linac isocenter with a coronal field of view of approximately 18 cm in both the superior-inferior and left-right directions at isocenter. For soft tissue targets, the system is designed to be used with radio-opaque platinum markers implanted near the target. Two markers, 2 cm away from each other and placed close enough to the target anatomy so that they could be observed within the field of view of the x-ray localization system at the time of treatment, were implanted prior to CT imaging and treatment planning,. Specific patient breathing characteristics were determined during 4D CT. If the breathing pattern was adequate, respiratory-gated delivery (turning the beam on only at a specified phase of respiration) was used. This method "freezes" target motion and allows reduction of beam margins, thereby reducing the amount of irradiated normal tissue. The Novalis system is well suited to gated delivery and has been evaluated extensively by Tenn et al (Tenn, Solberg, and Medin 2005). The following is a brief procedural summary from that work which is incorporated into this study: The patient is set up in the treatment room and infrared reflective markers with adhesive bases are attached to their anterior surface so that breathing motion can be monitored. A second set of infrared reflective markers is rigidly attached to the treatment couch and used as a reference against which the movement of patient markers is measured. These rigidly mounted reflectors are also used to track couch location during the patient positioning process. The 3D movement of the patient's anterior surface is tracked via the infrared markers and the anterior-posterior component of this trajectory is used to monitor breathing motion. The system plots breathing motion versus time and a reference level is specified on this breathing trace. This designates the point in the breathing trace at which the verification x-ray images will be triggered. The two images are obtained sequentially at the instant the breathing trace crosses this level during exhale phase. Because the patient is localized based on these images, the gating level is set at the same phase in the breathing cycle at which the planning CT data was obtained. Within each image the user locates the positions of the implanted markers. From these positions the system reconstructs the 3D geometry of the implanted markers and determines the shifts necessary to bring them into alignment with the planning CT. The patient is subsequently positioned according to the calculated shifts. Finally, a gating window (beam-on region) during which the linac beam will be delivered is selected about the reference level. The system can gate the beam in both inhale and exhale phases of the breathing cycle. Subsequent x-ray images verifying the location of the implanted markers are obtained at the gating level continuously during treatment. If marker positions remain within tolerance limits, the target position may also be assumed to be correctly positioned. If they are outside the limit, the newly obtained images can be used to reposition the patient and maintain treatment accuracy.

2.2.5 Dose computation

The treatment plan used for each patient was based on an analysis of the volumetric dose, including dose volume histogram (DVH) analyses of the PTV and critical normal structures. Treatment planning was accomplished with multiple coplanar conformal beams or arcs to allow for a high degree of dose conformality. The uniformity requirement is +10%/-5% of the total dose at the prescription point within the tumor volume. The IMRT was used if it was of benefit for decreasing tissue complications. Beam's Eye View techniques were used to select the beam isocenter and direction to fully encompass the target volume while minimizing the inclusion of the critical organs in order to select the plan that minimizes the dose to normal tissues.

2.2.6 Dose specification

A 5-fraction dose was prescribed. The prescription dose was the isodose which encompasses at least 95% of PTV. DVHs were generated for all critical organs-at-risk. The dose to the kidneys was carefully monitored and kidney volumes were defined on simulation fields. The percent of total kidney volume (defined as the sum of the left and right kidney volumes) receiving 15 Gy (3 Gy per fraction) was required to be less than 35% of the total kidney volume. The maximum dose to any point within the spinal cord was not allowed to exceed 15 Gy (3 Gy per fraction). At least 700 ml or 35% of normal liver was required to receive a total dose less than 15 Gy (3 Gy per fraction). The maximum point dose to the stomach or small bowel except duodenum could not exceed 60% of prescription dose. An isodose distribution of the treatment at the central axis view indicating the position of kidneys, liver and spinal cord was required. Dose homogeneity was defined as follows: No more than 20% of PTV receive >110% of its prescribed dose; No more than 1% of PTV receive <93% of its prescribed dose; No more than 1% or 1 cc of the tissue outside the PTV receive >110% of the dose prescribed to the PTV.

2.2.7 Daily target verification

The locations of the implanted markers were verified on daily Exac-Trac X-Rays prior to the delivery of stereotactic body radiation therapy.

2.3 Statistical analysis

For each patient, the mean and standard deviation of daily 3-dimensional position shifts (lateral, longitudinal and vertical) were measured. The systematic error (the mean of all patients' means) and the random error (the standard deviation around the systemic error) were calculated for daily patient position shifts. The amplitude changes and variability in amplitude changes were also measured. Multivariate logistic regression was used to analyze the effect of patients' BMI on patient position changes. All statistical calculations were performed using SAS 9.2 (SAS Institute Inc., Cary, North Carolina, USA).

3. Results

3.1 Systematic and random daily couch shifts

A total of 127 treatments from 26 patients were studied. Table 1 provides a summary of the systematic and random couch shifts using implanted internal markers. The entire group mean (systematic) and standard deviation (random) of the couch shifts from the body surface markers are -0.4 ± 5.6 mm, -1.3 ± 6.6 mm and -0.3 ± 4.7 mm in lateral (left-right), longitudinal (superior-inferior) and vertical (anterior-posterior) directions, respectively. The mean systematic couch shifts > 0 occur in (13/26) 50%, (12/26) 46% and (10/26) 38% in the left-right, superior-inferior and anterior-posterior directions, respectively. The mean random couch shifts > 5mm occur in (7/26) 27%, (12/26) 46% and (5/26) 19% in the left-right, superior-inferior and anterior-posterior directions, respectively. The mean systematic couch shifts are significantly smaller than the mean random couch shifts in left-right (-0.3 ± 3.6 mm vs. 4.1 ± 2.8 mm, $p < 0.0001$), superior-inferior (-1.1 ± 4.1 mm vs. 5.5 ± 3.2 mm, $p < 0.0001$) and anterior-posterior (-0.1 ± 3.1 mm vs. 3.5 ± 2.0 mm, $p < 0.0001$) directions, respectively. The couch shifts for the majority of fractions are within ± 10 mm (Figure 1A-1C)

	Systematic Error Mean (mm) ± SD	Random Error Mean (mm) ± SD	P (X^2)
Lateral shift	**-0.3 ± 3.6**	**4.1 ± 2.8**	**<0.0001**
Longitudinal shift	**-1.1 ± 4.1**	**5.5 ± 3.2**	**<0.0001**
Vertical shift	**-0.1 ± 3.1**	**3.5 ± 2.0**	**<0.0001**

Table 1. The averages of systematic and random daily couch shifts three-dimensionally

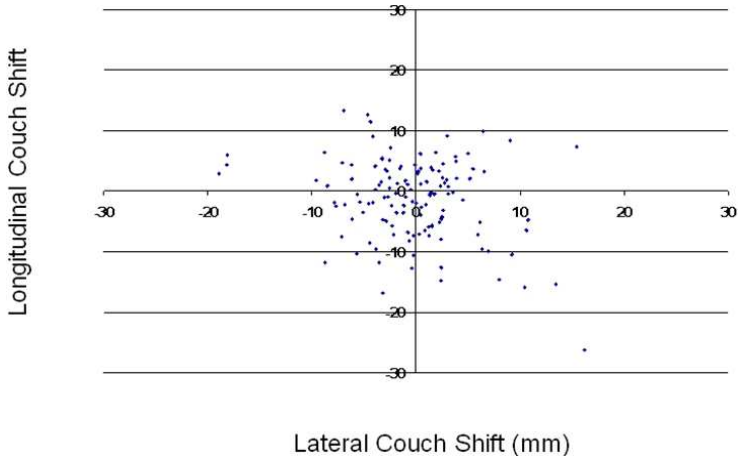

Fig. 1A. Longitudinal vs. Lateral couch shifts

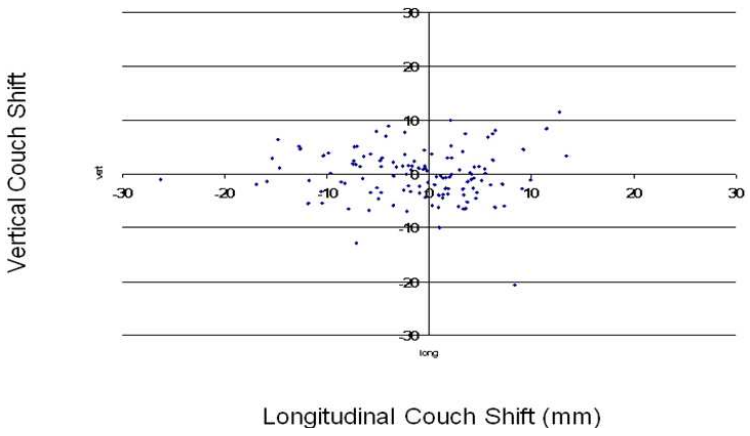

Fig. 1B. Vertical vs. Longitudinal couch shifts

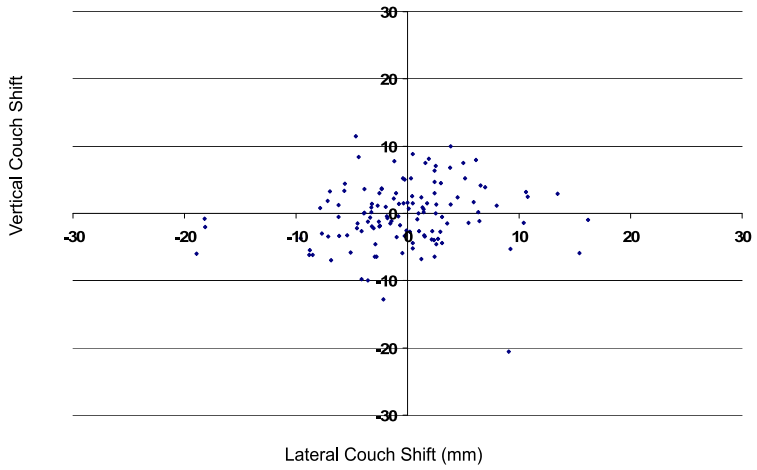

Fig. 1C. Vertical vs. Lateral couch shifts

3.2 Absolute systematic and random daily couch shifts

The amplitudes of the systemic and random daily couch shifts are summarized in table 2. The mean amplitudes of systematic couch shifts are significantly larger than the mean amplitude of random couch shift in left-right (4.1 ± 2.9 mm vs. 2.5 ± 1.3 mm, p = 0.015), superior-inferior (5.2 ± 3.1 mm vs. 3.2 ± 1.6 mm, p = 0.007) and anterior-posterior (3.6 ± 1.5 mm vs. 2.5 ± 1.6 mm, p = 0.016) directions, respectively. The amplitudes of couch shifts in the superior-inferior direction are significantly larger than those in the left-right (p = 0.045) or anterior-posterior directions (p = 0.001). The absolute couch shifts ≤ 3 mm, ≤ 5 mm and ≤ 10 mm occur in (51%, 71% and 93%), (37%, 60% and 87%) and (51%, 73% and 98%) in the left-right, superior-inferior and anterior-posterior directions, respectively (Figure 2A-2F). There is no correlation among 3 dimensional couch shifts (Figure 3A-3C).

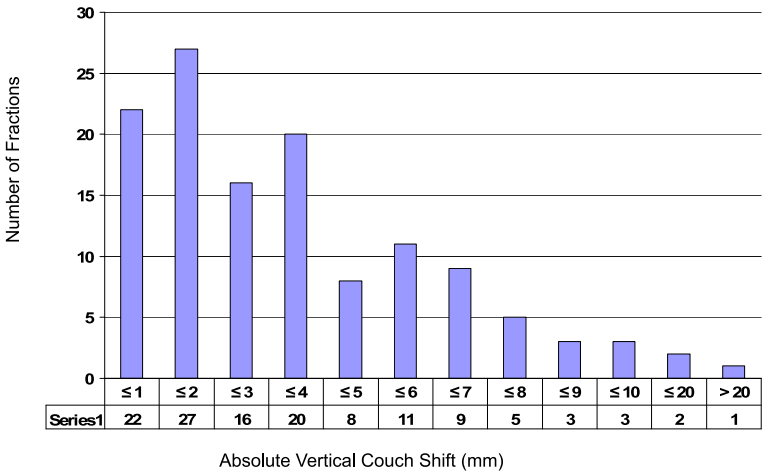

Fig. 2A. Distribution of absolute vertical couch shifts

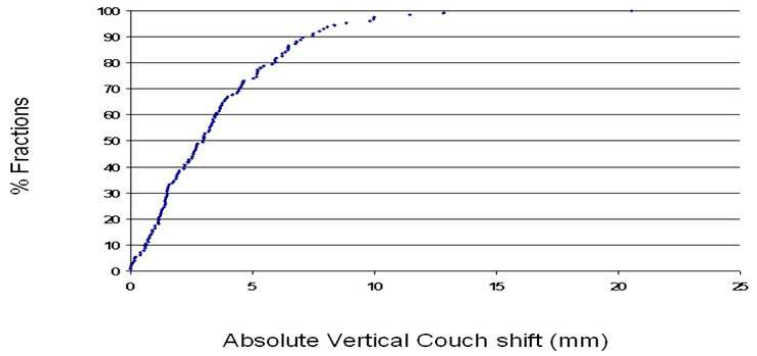

Fig. 2B. Cumulative distribution of absolute vertical couch shifts

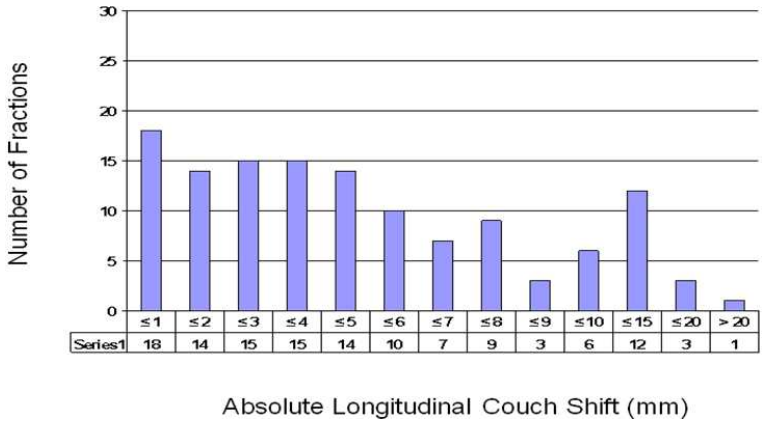

Fig. 2C. Distribution of absolute longitudinal couch shifts

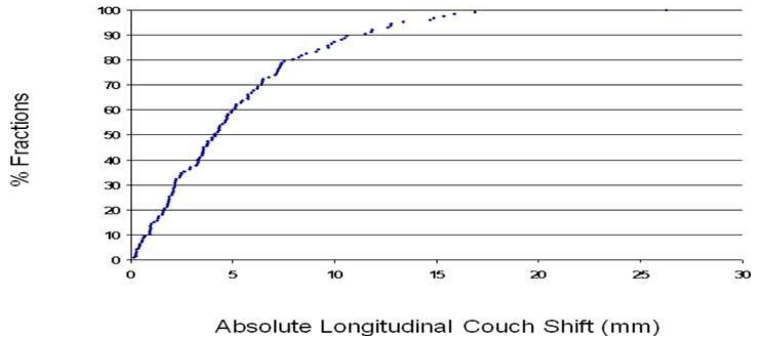

Fig. 2D. Cumulative distribution of absolute longitudinal couch shifts

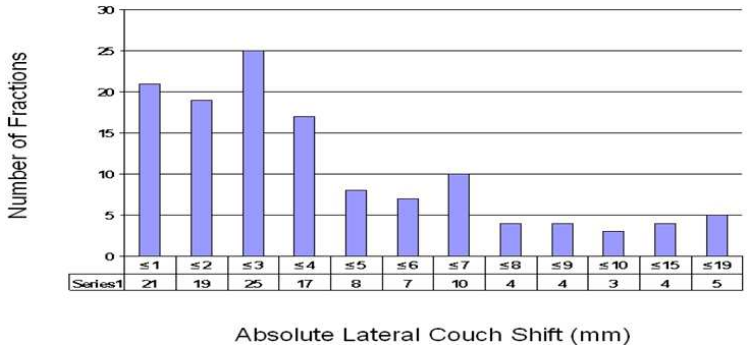

Fig. 2E. Distribution of absolute lateral couch shifts

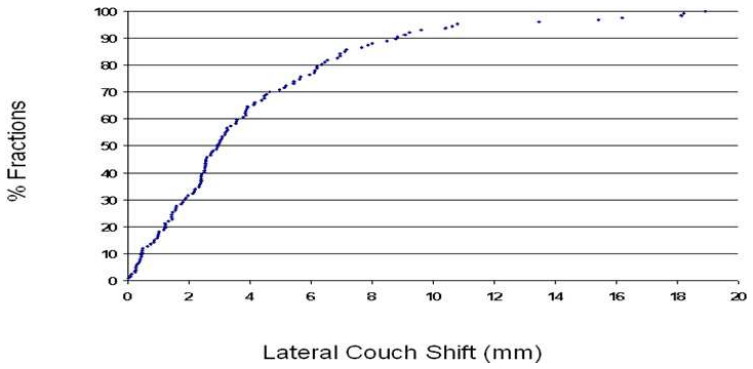

Fig. 2F. Cumulative distribution of absolute lateral couch shifts

Absolute Value (Amplitude)	Systematic Error Mean (mm) ± SD	Random Error Mean (mm) ± SD	P (X^2)
Lateral shift	4.1 ± 2.9	2.5 ± 1.3	0.015
Longitudinal shift	5.2 ± 3.1	3.2 ± 1.6	0.007
Vertical shift	3.6 ± 1.6	2.5 ± 1.6	0.016

Table 2. The averages of absolute systematic and random daily couch shifts three-dimensionally

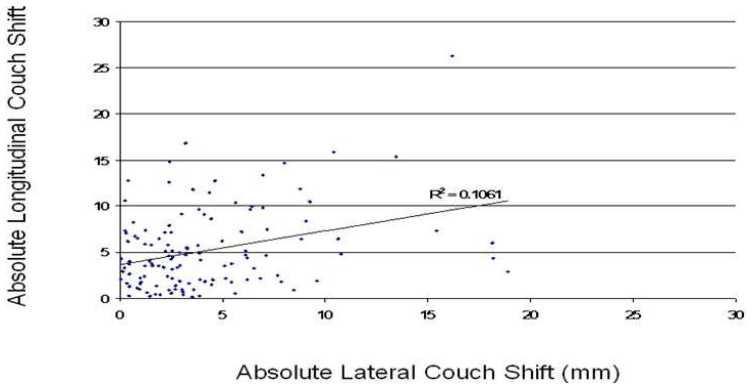

Fig. 3A. Absolute longitudinal vs. absolute lateral couch shifts

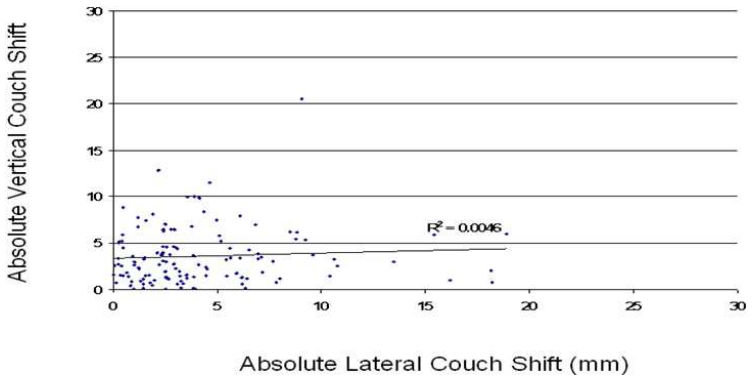

Fig. 3B. Absolute vertical vs. absolute lateral couch shifts

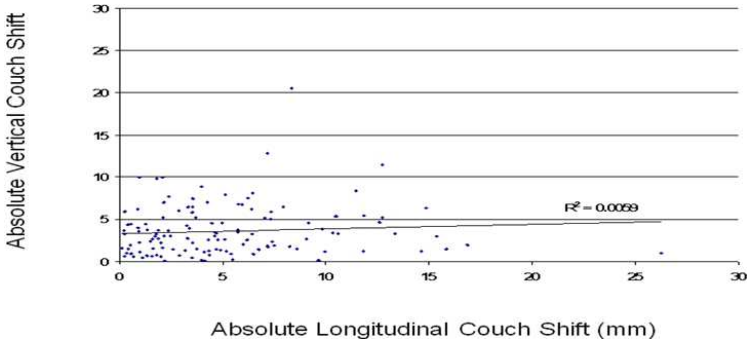

Fig. 3C. Absolute vertical vs. absolute longitudinal couch shifts

3.3 The magnitude of the pancreatic tumor motion vs. the amplitude of setup correction

Inter-fraction variability in the position of pancreatic tumors is generally considered to be resultant from pancreatic breathing motion and patient positioning. We examined the association of the magnitude of the changes in the pancreatic tumor breathing motion in 50% and 80% inhale and exhale with the amplitude of daily setup error correction and found no correlation between them ($R^2 \leq 0.012$). (Figure 4A-4C)

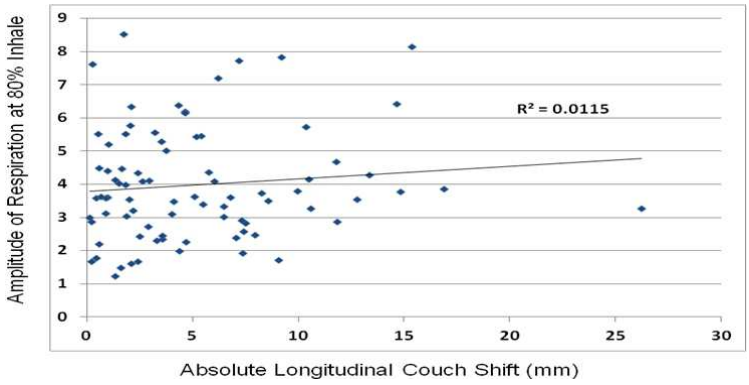

Fig. 4A. Relationship between amplitude of respiration and setup correction in the longitudinal direction

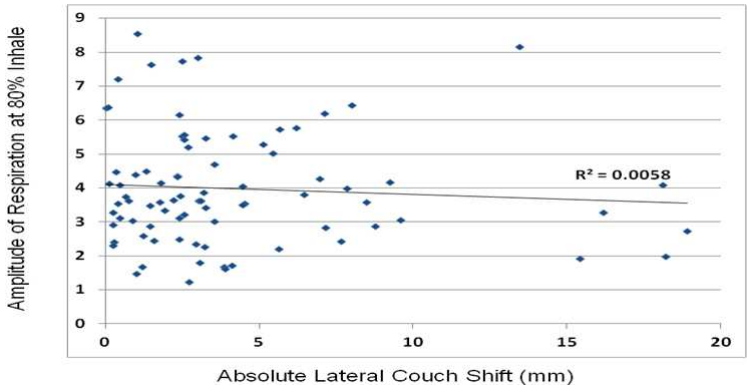

Fig. 4B. Relationship between amplitude of respiration and setup correction in the lateral direction

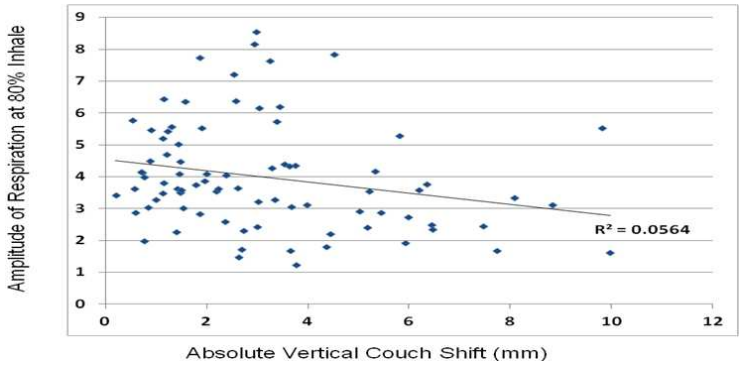

Fig. 4C. Relationship between amplitude of respiration and setup correction in the vertical direction

3.4 The effect of body mass index on daily couch shifts

The median age for this group of patients is 60 years old (range: 34 -79). Slightly more than half of the patients (14/26) are males. The BMIs for this group of patients range between 20 and 46 with a median value of 27 (kg/m²). There are 8 patients with BMIs of 20-25 and 18 patients with the BMIs of 26-46. Table 3 shows that there is no difference in daily couch shift distribution between these two groups based on BMIs of > 25 or ≤ 25.

	BMI 20-25 N (%)	BMI 26-46 N (%)	P (X^2)
Lateral systematic shift			**0.395**
≤ 0	**5 (62.5)**	**8 (44.4)**	
> 0	**3 (37.5)**	**10 (55.6)**	
Longitudinal systematic shift			**0.793**
≤ 0	**4 (50)**	**10 (55.6)**	
> 0	**4 (50)**	**8 (44.4)**	
Vertical systematic shift			**0.070**
≤ 0	**7 (87.5)**	**9 (50)**	
> 0	**1 (12.5)**	**9 (50)**	
Lateral random shift			**0.418**
≤ 5 mm	**5 (62.5)**	**14 (77.8)**	
> 5 mm	**3 (37.5)**	**4 (22.2)**	
Longitudinal random shift			**0.555**
≤ 5 mm	**5 (62.5)**	**9 (50)**	
> 5 mm	**3 (37.5)**	**9 (50)**	
Vertical random shift			**0.562**
≤ 5 mm	**7 (87.5)**	**14 (77.8)**	
> 5 mm	**1 (12.5)**	**4 (22.2)**	

Table 3. Distributions of daily couch shifts in patients with body mass indexes of > 25 and ≤ 25

Table 4 shows the results of multivariate regression analysis, revealing that patients with a BMI ≤ 25 are less likely to have an anterior vertical couch shift from the initial positioning (OR: 0.35, 95% CI: 0.16-0.77, p = 0.009) than those with a BMI > 25 after adjusting for age and gender, suggesting less correction is needed due to less body relaxation and skin movement in patients with a BMI ≤ 25 (kg/m^2) than those with a BMI > 25. BMI has no effect on the left-right or superior-inferior couch shifts.

BMI 20-25 vs. BMI 26-46	Odd Ratio (95% CI)	P (X^2)
Lateral systematic shift	0.787 (0.371-1.671)	0.533
Longitudinal systematic shift	1.384 (0.657-2.914)	0.393
Vertical systematic shift	0.351 (0.160-1.773)	0.009
Lateral random shift	2.087 (0.333-13.077)	0.432
Longitudinal random shift	0.606 (0.105-3.513)	0.577
Vertical random shift	0.501 (0.043-5.838)	0.581

Table 4. The effect of body mass index on daily couch shifts by multivariate logistic regression analysis

Factors included in the regression models are age, gender and BMI.

4. Discussion

Accurate and precise patient positioning at the time of delivering stereotactic body radiotherapy is crucial. Image-guided respiratory-gated radiation therapy has been a major advancement in minimizing inter- and intra- fractional target variations. To minimize and correct for setup uncertainties and inter-fractional motion of extracranial tumors, various immobilization and localization techniques have been clinically implemented, including transabdominal ultrasonography (Lattanzi et al. 1999; Chandra et al. 2003; Langen et al. 2003), megavoltage imaging (Schiffner et al. 2007; Serago et al. 2006), kilovoltage imaging (Jaffray et al. 1999; Kupelian et al. 2008), use of an in-room computed tomography (CT)–linear accelerator system (Court et al. 2003; Wong et al. 2005), cone-beam CT (Jaffray et al. 1999; Kupelian et al. 2008), and placement of internal fiducials (Kupelian et al. 2008; Chen et al. 2007; Chung et al. 2004). Pancreatic tumor targets usually exhibit inter-fractional motion relative to the bony anatomy because of daily variation in stomach and duodenal filling and respiratory patterns. The bony anatomy can be imaged and aligned using in-room kilovoltage X-rays; however, with this approach, the position of the pancreatic tumor with respect to the bony anatomy is uncertain. Jayachandran et al. has compared the inter-fractional variation in pancreatic tumor position using bony anatomy to implanted fiducial markers and observed substantial residual uncertainty after alignment to bony anatomy when irradiating pancreatic tumors using respiratory gating (Jayachandran et al. 2010). They reported that bony anatomy matched tumor position in only 20% of the radiation treatments. This study evaluates the use of implanted platinum markers in pancreatic cancer

patients for daily setup correction. We acquired treatment planning CT scans at least 1 week after two fiducial markers were implanted to allow time for inflammation or edema to subside. The positions of these markers were then used to guide the daily patient setup correction.

4.1 The magnitude of the inter-fractional setup correction for pancreatic cancer

In this study, inter-fractional shifts of > 5 mm are observed in 29%, 27% and 40% of fractions in left-right, anterior-posterior and superior-inferior directions. When we examined the percentage of fractions with the inter-fractional shifts of > 10 mm, we observed only 7% and 2% in the directions of left-right and anterior-posterior but 13% in the direction of superior-inferior. The median and maximum couch shifts are 4.2 and 26.2 mm, 3.0 and 20.5 mm and 3.0 and 18.9 mm in superior-inferior, anterior-posterior and left-right directions, respectively. The couch shift in the superior-inferior direction is significantly larger than that in the anterior-posterior ($p = 0.001$) and left-right ($p = 0.045$) directions. There is no difference in couch shifts between anterior-posterior and left-right directions ($p = 0.22$). (Table 5)

Shifts	Median (mm)	Maximum (mm)	≤ 3 mm N (%)	≤ 5 mm N (%)	≤ 10 mm N (%)	T-test
Left-Right	3.0	18.9	65/127 (51)	90/127 (71)	118/127 (93)	SI vs. LR p=0.001
Superior-Inferior	4.2	26.2	47/127 (37)	76/127 (60)	111/127 (87)	SI vs. AP p=0.045
Anterior-Posterior	3.0	20.5	65/127 (51)	93/127 (73)	124/127 (98)	LR vs. AP p=0.216

Table 5. Comparison of the amplitudes of three-dimensional shifts in median, maximum, 3 mm, 5 mm and 10 mm.

There is no correlation in either the direction or the amplitude of couch shifts among all three directions. In contrast to our findings, Jayachandran et al. reported that the maximum shifts needed in the anterior-posterior, left-right, and superior-inferior directions were 9 mm, 13 mm, and 19 mm, respectively when fiducial markers were used which are smaller than what we found in the current study (Jayachandran et al. 2010). On the other hand, some earlier studies have shown much larger inter-fractional pancreatic motions of up to 40 mm (Booth and Zavgorodni 1999; Horst et al. 2002). Allen et al. reported a maximum of 17.7 mm inter-fractional setup error in pancreatic cancer using daily on line CT scan images (Li et al. 2007). Feng et al. characterized pancreatic tumor motion using CINE MRI and found that tumor borders moved much more than expected. They indicated that to provide 99% geometric coverage, margins of 20mm inferiorly, 10 mm anteriorly, 7 mm superiorly, and 4 mm posteriorly are required if respiratory gating is not used (Feng et al. 2009).

4.2 Relationship between setup correction and amplitude of pancreatic tumor breathing motion

To our knowledge, this is the first study to evaluate the correlation of the amplitude of respiration to patient position displacement in pancreatic cancer. We did not find any association between the magnitude of the changes in the pancreatic tumor breathing motion and the amplitude of daily setup error correction. This is consistent with the results reported by Case et al. for liver tumors (Case et al. 2009).

4.3 Effect of body mass index on setup correction

This is the first study to examine the influence of BMI on setup correction for pancreatic cancer. We observed that patients with a BMI of > 25 have a greater possibility of needing vertical setup correction than those with a BMI of ≤ 25. On the other hand, BMI has no effect on the setup corrections in superior-inferior and left-right directions. Worm et al reported that intrafractional errors for liver and lung cancer were independent of patient's BMI (Worm et al.). A study on generic planning target margin for rectal cancer treatment setup variation did show that BMI was significantly associated with systemic superior-inferior ($p<0.05$) and anterior-posterior ($p<0.01$) variation and random left-right variation ($p<0.05$) (Robertson, Campbell, and Yan 2009).

5. Conclusion

Daily alignment using fiducial markers is an effective method of localizing pancreas displacement. It provides the option of reducing margins, thus limiting normal tissue toxicity and allowing the possibility of dose escalation for better long-term control. For those patients without daily image guided set-up correction, margins of |mean| + 2|standard deviation| (11.6 mm, 14.5 mm, and 9.7 mm in left-right, superior-inferior, and anterior-posterior directions, respectively) should be added to the planning target volume. Patients with BMI >25 (kg/m^2) may need a larger anterior-posterior margin for planning target volume than those with BMI ≤ 25 (kg/m^2).

6. Abbreviations

US: United States
ACS: American Cancer Society
5-FU: 5-Fluorouracil
ECOG: The Eastern Cooperative Oncology Group
CT: computed tomography
4D CT: 4 dimensional computed tomography
MRI: Magnetic resonance imaging
FDG PET: fluorodeoxyglucose Positron emission tomography
GTV: Gross tumor volume
CTV: Clinical target volume
PTV: Planning target volume
DVH: Dose volume histogram
IMRT: Intensity modulated radiation therapy
SD: Standard deviation
BMI: Body mass index

7. References

ACS. 2011, Cancer Facts& Figures, http://www.cancer.org/acs/groups/content/@epidemiologysurveilance/documents/document/acspc-029771.pdf.

Booth, J. T., and S. F. Zavgorodni. 1999. "Set-up error & organ motion uncertainty: a review." Australas Phys Eng Sci Med no. 22 (2):29-47.

Breslin, T. M., K. R. Hess, D. B. Harbison, M. E. Jean, K. R. Cleary, A. P. Dackiw, R. A. Wolff, J. L. Abbruzzese, N. A. Janjan, C. H. Crane, J. N. Vauthey, J. E. Lee, P. W. Pisters, and D. B. Evans. 2001. "Neoadjuvant chemoradiotherapy for adenocarcinoma of the pancreas: treatment variables and survival duration." Ann Surg Oncol no. 8 (2):123-32.

Bujko, K., M. P. Nowacki, A. Nasierowska-Guttmejer, W. Michalski, M. Bebenek, and M. Kryj. 2006. "Long-term results of a randomized trial comparing preoperative short-course radiotherapy with preoperative conventionally fractionated chemoradiation for rectal cancer." Br J Surg no. 93 (10):1215-23.

Case, R. B., J. J. Sonke, D. J. Moseley, J. Kim, K. K. Brock, and L. A. Dawson. 2009. "Inter- and intrafraction variability in liver position in non-breath-hold stereotactic body radiotherapy." Int J Radiat Oncol Biol Phys no. 75 (1):302-8.

Chandra, A., L. Dong, E. Huang, D. A. Kuban, L. O'Neill, I. Rosen, and A. Pollack. 2003. "Experience of ultrasound-based daily prostate localization." Int J Radiat Oncol Biol Phys no. 56 (2):436-47.

Chen, J., R. J. Lee, D. Handrahan, and W. T. Sause. 2007. "Intensity-modulated radiotherapy using implanted fiducial markers with daily portal imaging: assessment of prostate organ motion." Int J Radiat Oncol Biol Phys no. 68 (3):912-9.

Chung, P. W., T. Haycocks, T. Brown, Z. Cambridge, V. Kelly, H. Alasti, D. A. Jaffray, and C. N. Catton. 2004. "On-line aSi portal imaging of implanted fiducial markers for the reduction of interfraction error during conformal radiotherapy of prostate carcinoma." Int J Radiat Oncol Biol Phys no. 60 (1):329-34.

Court, L., I. Rosen, R. Mohan, and L. Dong. 2003. "Evaluation of mechanical precision and alignment uncertainties for an integrated CT/LINAC system." Med Phys no. 30 (6):1198-210.

Evans DBAJ, Willett CG. . 2011. Cancer of the pancreas. Edited by Rosenberg SA DeVita VT Jr HS. 1 vols. Vol. 1, Cancer principles and practice of oncology. New York: Lippincott Williams & Wilkins.

Feng, M., J. M. Balter, D. Normolle, S. Adusumilli, Y. Cao, T. L. Chenevert, and E. Ben-Josef. 2009. "Characterization of pancreatic tumor motion using cine MRI: surrogates for tumor position should be used with caution." Int J Radiat Oncol Biol Phys no. 74 (3):884-91.

Guckenberger, M., J. Meyer, J. Wilbert, K. Baier, G. Mueller, J. Wulf, and M. Flentje. 2006. "Cone-beam CT based image-guidance for extracranial stereotactic radiotherapy of intrapulmonary tumors." Acta Oncol no. 45 (7):897-906.

Herfarth, K. K., J. Debus, F. Lohr, M. L. Bahner, P. Fritz, A. Hoss, W. Schlegel, and M. F. Wannenmacher. 2000. "Extracranial stereotactic radiation therapy: set-up accuracy

of patients treated for liver metastases." Int J Radiat Oncol Biol Phys no. 46 (2):329-35.

Horst, E., O. Micke, C. Moustakis, A. Schuck, U. Schafer, and N. A. Willich. 2002. "Conformal therapy for pancreatic cancer: variation of organ position due to gastrointestinal distention--implications for treatment planning." Radiology no. 222 (3):681-6.

Jaffray, D. A., D. G. Drake, M. Moreau, A. A. Martinez, and J. W. Wong. 1999. "A radiographic and tomographic imaging system integrated into a medical linear accelerator for localization of bone and soft-tissue targets." Int J Radiat Oncol Biol Phys no. 45 (3):773-89.

Jayachandran, P., A. Y. Minn, J. Van Dam, J. A. Norton, A. C. Koong, and D. T. Chang. 2010. "Interfractional uncertainty in the treatment of pancreatic cancer with radiation." Int J Radiat Oncol Biol Phys no. 76 (2):603-7.

Klinkenbijl, J. H., J. Jeekel, T. Sahmoud, R. van Pel, M. L. Couvreur, C. H. Veenhof, J. P. Arnaud, D. G. Gonzalez, L. T. de Wit, A. Hennipman, and J. Wils. 1999. "Adjuvant radiotherapy and 5-fluorouracil after curative resection of cancer of the pancreas and periampullary region: phase III trial of the EORTC gastrointestinal tract cancer cooperative group." Ann Surg no. 230 (6):776-82; discussion 782-4.

Koong, A. C., Q. T. Le, A. Ho, B. Fong, G. Fisher, C. Cho, J. Ford, J. Poen, I. C. Gibbs, V. K. Mehta, S. Kee, W. Trueblood, G. Yang, and J. A. Bastidas. 2004. "Phase I study of stereotactic radiosurgery in patients with locally advanced pancreatic cancer." Int J Radiat Oncol Biol Phys no. 58 (4):1017-21.

Kupelian, P. A., C. Lee, K. M. Langen, O. A. Zeidan, R. R. Manon, T. R. Willoughby, and S. L. Meeks. 2008. "Evaluation of image-guidance strategies in the treatment of localized prostate cancer." Int J Radiat Oncol Biol Phys no. 70 (4):1151-7.

Langen, K. M., J. Pouliot, C. Anezinos, M. Aubin, A. R. Gottschalk, I. C. Hsu, D. Lowther, Y. M. Liu, K. Shinohara, L. J. Verhey, V. Weinberg, and M. Roach, 3rd. 2003. "Evaluation of ultrasound-based prostate localization for image-guided radiotherapy." Int J Radiat Oncol Biol Phys no. 57 (3):635-44.

Lattanzi, J., S. McNeeley, W. Pinover, E. Horwitz, I. Das, T. E. Schultheiss, and G. E. Hanks. 1999. "A comparison of daily CT localization to a daily ultrasound-based system in prostate cancer." Int J Radiat Oncol Biol Phys no. 43 (4):719-25.

Li, X. A., X. S. Qi, M. Pitterle, K. Kalakota, K. Mueller, B. A. Erickson, D. Wang, C. J. Schultz, S. Y. Firat, and J. F. Wilson. 2007. "Interfractional variations in patient setup and anatomic change assessed by daily computed tomography." Int J Radiat Oncol Biol Phys no. 68 (2):581-91.

Oettle, H., S. Post, P. Neuhaus, K. Gellert, J. Langrehr, K. Ridwelski, H. Schramm, J. Fahlke, C. Zuelke, C. Burkart, K. Gutberlet, E. Kettner, H. Schmalenberg, K. Weigang-Koehler, W. O. Bechstein, M. Niedergethmann, I. Schmidt-Wolf, L. Roll, B. Doerken, and H. Riess. 2007. "Adjuvant chemotherapy with gemcitabine vs observation in patients undergoing curative-intent resection of pancreatic cancer: a randomized controlled trial." Jama no. 297 (3):267-77.

Pisters, P. W., J. L. Abbruzzese, N. A. Janjan, K. R. Cleary, C. Charnsangavej, M. S. Goswitz, T. A. Rich, I. Raijman, R. A. Wolff, R. Lenzi, J. E. Lee, and D. B. Evans. 1998. "Rapid-

fractionation preoperative chemoradiation, pancreaticoduodenectomy, and intraoperative radiation therapy for resectable pancreatic adenocarcinoma." J Clin Oncol no. 16 (12):3843-50.

Pisters, P. W., W. A. Hudec, J. E. Lee, I. Raijman, S. Lahoti, N. A. Janjan, T. A. Rich, C. H. Crane, R. Lenzi, R. A. Wolff, J. L. Abbruzzese, and D. B. Evans. 2000. "Preoperative chemoradiation for patients with pancreatic cancer: toxicity of endobiliary stents." J Clin Oncol no. 18 (4):860-7.

Regine, W. F., K. A. Winter, R. A. Abrams, H. Safran, J. P. Hoffman, A. Konski, A. B. Benson, J. S. Macdonald, M. R. Kudrimoti, M. L. Fromm, M. G. Haddock, P. Schaefer, C. G. Willett, and T. A. Rich. 2008. "Fluorouracil vs gemcitabine chemotherapy before and after fluorouracil-based chemoradiation following resection of pancreatic adenocarcinoma: a randomized controlled trial." Jama no. 299 (9):1019-26.

Robertson, J. M., J. P. Campbell, and D. Yan. 2009. "Generic planning target margin for rectal cancer treatment setup variation." Int J Radiat Oncol Biol Phys no. 74 (5):1470-5.

Schiffner, D. C., A. R. Gottschalk, M. Lometti, M. Aubin, J. Pouliot, J. Speight, I. C. Hsu, K. Shinohara, and M. Roach, 3rd. 2007. "Daily electronic portal imaging of implanted gold seed fiducials in patients undergoing radiotherapy after radical prostatectomy." Int J Radiat Oncol Biol Phys no. 67 (2):610-9.

Serago, C. F., S. J. Buskirk, T. C. Igel, A. A. Gale, N. E. Serago, and J. D. Earle. 2006. "Comparison of daily megavoltage electronic portal imaging or kilovoltage imaging with marker seeds to ultrasound imaging or skin marks for prostate localization and treatment positioning in patients with prostate cancer." Int J Radiat Oncol Biol Phys no. 65 (5):1585-92.

Sonke, J. J., J. Lebesque, and M. van Herk. 2008. "Variability of four-dimensional computed tomography patient models." Int J Radiat Oncol Biol Phys no. 70 (2):590-8.

Spitz, F. R., J. L. Abbruzzese, J. E. Lee, P. W. Pisters, A. M. Lowy, C. J. Fenoglio, K. R. Cleary, N. A. Janjan, M. S. Goswitz, T. A. Rich, and D. B. Evans. 1997. "Preoperative and postoperative chemoradiation strategies in patients treated with pancreaticoduodenectomy for adenocarcinoma of the pancreas." J Clin Oncol no. 15 (3):928-37.

Tenn, S. E., T. D. Solberg, and P. M. Medin. 2005. "Targeting accuracy of an image guided gating system for stereotactic body radiotherapy." Phys Med Biol no. 50 (23):5443-62.

Wong, J. R., L. Grimm, M. Uematsu, R. Oren, C. W. Cheng, S. Merrick, and P. Schiff. 2005. "Image-guided radiotherapy for prostate cancer by CT-linear accelerator combination: prostate movements and dosimetric considerations." Int J Radiat Oncol Biol Phys no. 61 (2):561-9.

Worm, E. S., A. T. Hansen, J. B. Petersen, L. P. Muren, L. H. Praestegaard, and M. Hoyer. "Inter- and intrafractional localisation errors in cone-beam CT guided stereotactic radiation therapy of tumours in the liver and lung." Acta Oncol no. 49 (7):1177-83.

Yeo CJ, Cameron JL, Sohn TA, Lillemoe KD, Pitt HA, Talamini MA, Hruban RH, Ord SE, Sauter PK, Coleman J, Zahurak ML, Grochow LB, Abrams RA. 1997. "Six hundred fifty consecutive pancreaticoduodenectomies in the 1990s: pathology, complications, and outcomes." Ann Surg no. 226:248-257.

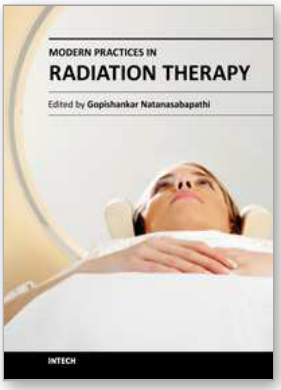

Modern Practices in Radiation Therapy

Edited by Dr. Gopishankar Natanasabapathi

ISBN 978-953-51-0427-8
Hard cover, 370 pages
Publisher InTech
Published online 30, March, 2012
Published in print edition March, 2012

Cancer is the leading cause of death in economically developed countries and the second leading cause of death in developing countries. It is an enormous global health encumbrance, growing at an alarming pace. Global statistics show that in 2030 alone, about 21.4 million new cancer cases and 13.2 million cancer deaths are expected to occur, simply due to the growth, aging of the population, adoption of new lifestyles and behaviors. Amongst the several modes of treatment for cancer available, Radiation treatment has a major impact due to technological advancement in recent times. This book discusses the pros and cons of this treatment modality. This book "Modern Practices in Radiation Therapy" has collaged topics contributed by top notch professionals and researchers all around the world.

How to reference

In order to correctly reference this scholarly work, feel free to copy and paste the following:

Chi Lin, Shifeng Chen and Michael J. Baine (2012). Stereotactic Body Radiotherapy for Pancreatic Adenocarcinoma: Set-Up Error Correction Using Internal Markers and It's Association with the Patient's Body Mass Index, Modern Practices in Radiation Therapy, Dr. Gopishankar Natanasabapathi (Ed.), ISBN: 978-953-51-0427-8, InTech, Available from: http://www.intechopen.com/books/modern-practices-in-radiation-therapy/stereotactic-body-radiotherapy-for-pancreatic-adenocarcinoma-set-up-error-correction-using-internal-

INTECH
open science | open minds

InTech Europe
University Campus STeP Ri
Slavka Krautzeka 83/A
51000 Rijeka, Croatia
Phone: +385 (51) 770 447
Fax: +385 (51) 686 166
www.intechopen.com

InTech China
Unit 405, Office Block, Hotel Equatorial Shanghai
No.65, Yan An Road (West), Shanghai, 200040, China
中国上海市延安西路65号上海国际贵都大饭店办公楼405单元
Phone: +86-21-62489820
Fax: +86-21-62489821